

# Unsteady Aerodynamics and Dynamic Response of Flexible Supersonic Aircraft to Continuous Turbulence

JACK MORITO II\* AND KENNETH W. SIDWELL\*  
*The Boeing Company, Seattle, Wash.*

This paper presents an analytical evaluation of unsteady aerodynamic forces and dynamic response of a flexible airplane to continuous turbulence in supersonic flight by applying the power-spectral-density (PSD) method. A brief explanation of differences in observed upwashes arising from the elastic and the gust oscillations is given. The aerodynamics for supersonic flight is described in terms of lifting-surface theory represented by a linear integral equation. The development is carried out for an airplane with coplanar wings of arbitrary planform subjected to a random vertical turbulence description. By applying the box technique, the aerodynamic influence coefficients are obtained for the combined elastic response and gust excitation velocity potential, which in turn determines the aerodynamic loads and the generalized forces. Choosing the flexible modes as the natural modes of the free-free airplane vibration, the frequency response functions are then determined. The interpretation of statistical results and the definition of parameters obtained by the PSD method, which are useful for design purposes, are discussed. The method of calculating the gust excitation forces and response of a flexible airplane is demonstrated by numerical examples.

## Nomenclature

$A$	= integration area
$A^{m,n}$	= area of box, $m,n$
$a_{i,o}$	= magnitude factor of $i$ th mode
$b^{m,n}$	= chordwise dimension of box, $m,n$
$b_c$	= chordwise dimension of Mach box
$b_r$	= reference length such as box chordwise dimension or wing semi-span
$\bar{C}$	= damping-force coefficient
$\bar{F}_g$	= gust-force coefficient
$g_i$	= structure damping factor of $i$ th mode
$H$	= frequency response function
$\bar{K}$	= stiffness-force coefficient
$k_r$	= reduced frequency $\omega b_r / U$
$L$	= scale of turbulence
$M$	= Mach number
$\bar{M}$	= inertia force coefficient
$M_i$	= generalized mass for $i$ th mode
$P$	= pressure
$Q_i$	= generalized force
$q$	= dynamic pressure
$q_i$	= generalized coordinate
$r_h$	= hyperbolic radius $[(x - \xi)^2 - \beta^2(y - \eta)^2]^{1/2}$
$S$	= wing area
$t$	= time
$U$	= uniform flow speed or airplane speed
$w$	= upwash
$W_g$	= gust vertical velocity
$x, y, z$	= longitudinal, lateral, and vertical axes
$z_i(x,y)$	= $i$ th mode shape
$z(x,y,t;\omega)$	= displacement of point $(x,y)$ at time $t$ under gust frequency $\omega$
$\beta$	= $(M_\infty^2 - 1)^{1/2}$
$\rho$	= air density
$\sigma$	= rms value or standard deviation
$\Phi$	= PSD and velocity potential
$\omega$	= circular frequency and gust input frequency
$\omega_i$	= natural frequency of $i$ th mode
$\xi$	= coordinate in $x$ axis

$\eta$	= coordinate in $y$ axis
$\Omega$	= spatial frequency of turbulence, $2\pi/\lambda$
$\lambda$	= wavelength of turbulence
$\{ \}$	= column matrix
$[ \ ]$	= rectangular matrix

## Subscripts

$D$	= diaphragm
$i$	= $i$ th mode
$l$	= lower surface and leading edge
$o$	= non-time-dependent quantity, and output
$t$	= trailing edge
$u$	= upper surface
$\infty$	= uniform flow condition

## Superscripts

$E$	= structure term
$G$	= gust or turbulence
$m,n$	= value of box $m,n$
$( )^*$	= Hermitian matrix
$( )'$	= derivative w.r.t. spatial frequency
$( )$	= dimensionless quantity

## Introduction

CONTRARY to some earlier predictions, the existence of clear-air turbulence at altitudes above 50,000 ft, the cruising regime of supersonic aircraft, has been firmly established by recent WU-2 flights conducted by the Air Force. The supersonic aircraft, being characterized by low aspect-ratio, highly swept wings mounted on long flexible fuselage, must operate in this environment. Therefore, the need becomes apparent to investigate the response of the supersonic aircraft to continuous turbulence and evaluate its effect upon design loads, fatigue life, handling qualities, and crew and passenger comfort.

A description of continuous atmospheric turbulence for current jet-transport cruise altitudes has been extensively reported in the literature. This description contains measured gust power spectra for clear-air and storm turbulence and the statistical distribution of root-mean-square (rms) gust intensity for various altitudes from sea level to as high as 75,000 ft.

Presented at the AIAA/ASME 8th Structures, Structural Dynamics & Materials Conference, Palm Springs, Calif., March 29-31, 1967 (no paper number; published in bound volume of conference papers); submitted April 14, 1967; revision received November 30, 1967.

\* Research Engineer, Product Development Structure Staff, Commercial Airplane Division. Member AIAA.

The difficulties encountered in the analysis of the response of flexible airplanes to continuous turbulence are the effects caused by the pilot, autopilot, and stability augmentation systems. Although this paper does not include these effects, it is worthwhile noticing their importance for future consideration.

In the development that follows, a statistical description of atmospheric turbulence is assumed to have been established for the supersonic aircraft cruising-altitude range. The aerodynamics for supersonic flight is written in terms of lifting-surface theory represented by a linear integral equation.<sup>1</sup> The computation is carried out for aircraft with coplanar wings of arbitrary planform subjected to a random vertical turbulence description that accounts for randomness in space along the flight path. The total turbulence field is represented at a point on the lifting surface by the superposition of an infinite number of elementary waves of upwash velocities. In essence, these elementary waves are representative of the entire range of wavelength and orientation. The phase relation between the gust excitation forces and the elastic response forces is then discussed by applying the gust orientation angle.

The integral equation based on linear perturbation theory is arranged to solve for the combined elastic response and gust excitation velocity potential at a point by applying the box technique, which assumes that the upwash inside the box is constant. Utilization of the velocity potential determines the aerodynamic loads on the wing from which the generalized forces due to elastic response and gust excitation are computed. Choosing the flexible modes as the natural modes for the free-free airplane vibration, the frequency response function is then derived. The response spectrum of the structure is determined from the frequency response function and the turbulence spectrum.

The method of calculating the gust excitation forces and the airplane response is demonstrated by two numerical examples for supersonic aircraft flying at speeds of  $M_\infty = 2.5$  and  $2.7$  and cruising altitudes =  $65,000$  and  $61,000$  ft, respectively.

## Analysis of Supersonic Aerodynamic Forces

### Upwash on the Elastic Structure under the Gust

The upwash pattern on the wings, which are subjected to the atmospheric turbulence field, is obtained by the superposition of an infinite number of elementary waves of upwash velocities. Each gust component undergoes harmonic motion with the amplitude remaining invariant along the uniform streamwise direction (provided that the gust is one-dimensional and homogeneous), but whose phase is varied by  $\Omega(x_p - x_q)$  at the relative streamwise position of points  $P$  and  $Q$  (see Fig. 1). Conversely, the upwash velocities associated with the elastic deformation in the uniform flow  $M_\infty$  at  $P$  and  $Q$  are only different in their amplitudes but are in phase for the same mode. In the case of the elastic mode, certain points do not feel any deformation, i.e., the nodal points exist. However, the nodal points never exist for the gust input case. Thus, the resultant upwash at the wing surface due to the superposition of the gust field and structural response is given by

$$w(x, y, t; \omega) = \frac{\partial z(x, y, t)}{\partial t} + U \frac{\partial z(x, y, t)}{\partial x} +$$

$$W_{e,0}(\omega) \exp[i\omega(t - \frac{x-a}{U})] \quad (1)$$

where the wing elastic deformation is expressed by

$$z(x, y, t) = \sum_j^N z_j(x, y) q_j(t) = \sum_j^N z_j(x, y) a_{j,0} e^{i\omega t} \quad (2)$$

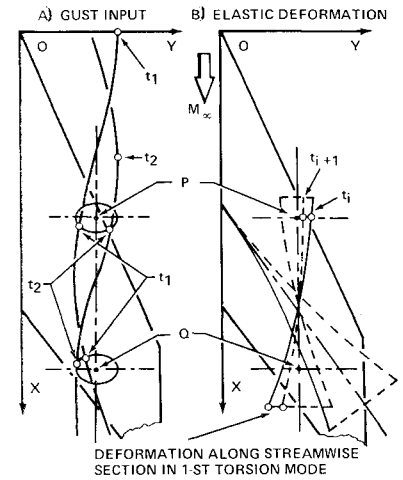


Fig. 1 Upwash oscillations due to gust and elastic oscillations.

and  $\omega a/U = \Omega a =$  initial gust orientation angle at  $t = 0$  and  $x = 0$ .

### Perturbation Potential of Elastic Structure under the Gust in Supersonic Flight

The surface perturbation potential at the point  $(x, y, 0+)$  of the wing in supersonic flow is obtained by integrating over the disturbed region bounded by the forward Mach lines emanating from that point. In the case of simple harmonic motion of a planar-form lifting surface, the up-surface potential at  $(x, y)$  is related to the complex upwash at  $(\xi, \eta)$  by the following integral equation<sup>2</sup>:

$$\Phi_0(x, y) e^{i\omega t} = - \frac{e^{i\omega t}}{\pi} \times \iint_A \frac{w_0(\xi, \eta; \omega) \exp[-i \frac{M_\infty^2 \omega}{U \beta^2} (x - \xi)] \cos \frac{M_\infty \omega}{U \beta^2} r_h}{r_h} d\xi d\eta \quad (3)$$

where  $A$  = area bounded by the forward Mach lines emanating from a point  $(x, y, 0+)$  and intersecting the wing leading edges (if supersonic L.E.) or the foremost wing nose Mach lines (if subsonic L.E.).

Applying the box technique, in which the upwash intensity is assumed to be constant inside the box, the potential difference at the center of box  $(m, n)$  denoted as  $\Delta\Phi(x_m, y_n)$  may be written symbolically as

$$\begin{aligned} \Delta\Phi_0(x_m, y_n) &= \Phi_u(x_m, y_n) - \Phi_l(x_m, y_n) \\ &= - \frac{2}{\pi} \sum_\nu \sum_\mu w_0(\xi, \eta) \times \\ &\quad \left\{ b_r \iint_{A(\nu, \mu)} \frac{\exp[-i \frac{k_r M_\infty^2}{\beta} (\bar{x}_m - \bar{\xi})] \cos \frac{k_r M_\infty}{\beta} \bar{r}_h}{r_h} d\xi d\eta \right\} \\ &\quad C_{\bar{\nu}\bar{\mu}} \end{aligned} \quad (4)$$

where

$C_{\bar{\nu}\bar{\mu}}$  = complex velocity influence coefficient which depends on gust frequency  $\omega$ , flight Mach number  $M_\infty$ , and relative location of "sending" and "receiving" boxes on wings

$\bar{\nu}, \bar{\mu} = n - \nu, m - \mu$ , respectively  
 $\bar{x}, \bar{\xi} = x/b_r, \xi/b_r$ , respectively, etc.

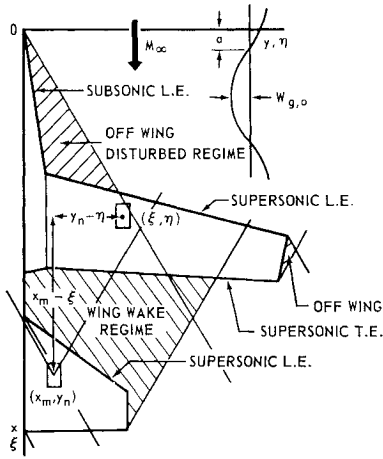


Fig. 2 Wing-edge boundary conditions.

Substitution of Eqs. (1) and (2) into Eq. (4) yields the velocity potential difference due to the  $j$ th elastic mode,

$$\Delta\Phi_j^E(x_m, y_n) = \frac{b_r}{\beta} U e^{i\omega t} \sum_{\bar{\nu}} \sum_{\bar{\mu}} \left\{ \underbrace{b_r \frac{\partial z_j(x_{\bar{\nu}}, y_{\bar{\mu}})}{\partial x}}_{\text{elastic slope}} + \underbrace{ik_r z_j(x_{\bar{\nu}}, y_{\bar{\mu}})}_{\text{elastic deflection}} \right\} C_{\bar{\nu}\bar{\mu}} \frac{a_{j,o}}{b_r} \quad (5)$$

Similarly, the velocity potential difference due to the gust input is

$$\Delta\Phi^G(x_m, y_n) = (b_r/\beta) U e^{i\omega t} e^{i\Omega\alpha} \times \underbrace{\sum_{\bar{\nu}} \sum_{\bar{\mu}} \left\{ b_r \frac{\cos\Omega x_{\bar{\nu}}}{b_r} + ik_r \frac{(-\sin\Omega x_{\bar{\nu}})}{k_r} \right\} C_{\bar{\nu}\bar{\mu}} \frac{W_{g,o}}{U}}_{\text{reference phase angle}} \quad (6)$$

pseudo wing slope      pseudo wing deflection

### Boundary Conditions

The boundary conditions for wing edges are classified as the following (see Fig. 2).

1) Purely supersonic leading-edge condition: The non-communicative character between the upper and lower surfaces does not cause any complexity.

2) Mixed supersonic leading-edge condition: To treat the case of a wing with a mixed supersonic leading edge, the Evvard concept is applied. In this concept, diaphragms of unknown upwashes are added to the given wing.<sup>1</sup> The off-wing diaphragm, which covers the region between the foremost Mach lines of the wing and the subsonic leading edge, results in a combined wing including the diaphragm planform area, which has completely supersonic edge. The upwash of the diaphragm, which is determined by applying the condition of zero velocity potential difference at the point, creates an additional contribution to the pressure at any point on the wing surface. Thus, for the diaphragm,

$$\Delta\Phi_D(x_m, y_n) = \sum_{\bar{\nu}} \sum_{\bar{\mu}} w_o(x_{\bar{\nu}}, y_{\bar{\mu}}) C_{\bar{\nu}\bar{\mu}} = 0$$

From this, the upwash at the diaphragm is

$$w_D(x_m, y_n) = \frac{\sum_{\substack{\bar{\nu} \neq m \\ \bar{\mu} \neq n}} C_{m-\bar{\mu}, n-\bar{\nu}} w(x_{\bar{\nu}}, y_{\bar{\mu}})}{C_{o,o}}$$

where the summation is performed for the region which is bounded by the forward Mach lines from a point  $(x_m, y_n)$  and the foremost wing nose Mach lines.

3) Between wing area and wing wake effect: For the wing wake area, we impose the following first-order approach. By analogy to the subsonic leading-edge area, there are no panels to support a pressure difference in the wing wake. Thus in the wake just after the trailing-edge area

$$\Delta P = \rho_{\infty} \frac{D\Delta\Phi}{Dt} = 0 \quad \text{or} \quad \frac{\partial\Delta\Phi}{\partial t} + U \frac{\partial\Delta\Phi}{\partial x} = 0 \quad (7)$$

The potential at  $x_w$  in the wake area is related to the just-after trailing edge by

$$\Delta\Phi(x_w, y, 0, t) = \Delta\Phi[x_i, y, 0, t - (x_w - x_i)/U] \quad (8)$$

Assuming a sinusoidally varying potential in the wake, the solution of differential equation (7) becomes

$$\Delta\Phi(x_w, y, 0, t; \omega) = \Delta\Phi(x_i, y, 0) \exp \left[ -ik_r \frac{x_w - x_i}{b_r} \right] e^{i\omega t} \quad (9)$$

Therefore, the problems for a sinusoidal gust input are well-posed and may be uniquely solved.

### Aerodynamic Forces Due to Gust Input

The pressure difference at station  $(x, y)$  and at time  $(t)$  is obtained from a linear superposition of both the elastic and gust potential contributions,

$$\Delta P^E(x, y, 0; t) = \sum_j \rho_{\infty} \left( \frac{\partial}{\partial t} + U \frac{\partial}{\partial x} \right) \Delta\Phi_j(x, y; t) = \rho_{\infty} \frac{b_r}{\beta} U^2 e^{i\omega t} \sum_j \left( ik_r + b_r \frac{\partial}{\partial x} \right) \overline{\Delta\Phi_j}(x, y; t) \frac{a_{j,o}}{b_r} \quad (10)$$

and

$$\Delta P^G(x, y, 0; t) = \rho_{\infty} \left( \frac{\partial}{\partial t} + U \frac{\partial}{\partial x} \right) \Delta\Phi^G(x, y; t) = \frac{b_r}{\beta} \rho_{\infty} U^2 e^{i\Omega\alpha} e^{i\omega t} \left( ik_r + b_r \frac{\partial}{\partial x} \right) \overline{\Delta\Phi^G}(x, y; t) \frac{W_{g,o}}{U} \quad (11)$$

Reference phase angle

Thus, the lift due to gust input (gust excitation force) is only rotated around the origin by the amount of reference phase angle  $\Omega\alpha$ .

### Generalized Forces Due to Gust Input

The generalized force over an area  $A(m, n)$  due to deformation in  $i$ th elastic mode and loading for the  $j$ th mode is

$$Q_{i,j,o}^{m,n} = \iint_{A(m,n)} z_i(x, y) \Delta P_{j,o}^E(x, y) dx dy = \frac{1}{2} \rho_{\infty} U^2 A^{m,n} \frac{2}{\beta} \left[ ik_r z_i^{m,n}(x, y) \overline{\Delta\Phi_{j,o}^{m,n}}(x, y) + \frac{b_r}{b_{m,n}} z_i^{m,n}(x, y) \{ \overline{\Delta\Phi_{j,o}^{m,n}}(x, y) \}_{x_i}^{x_t} - b_r \overline{\Delta\Phi_{j,o}^{m,n}}(x, y) \times \frac{\partial z_j(x, y)^{m,n}}{\partial x} \right] \frac{a_{j,o}}{b_r} \quad (12)$$

Similarly, the generalized force due to deformation in  $i$ th elastic mode and loading for gust excitation is

$$Q_{i,g,o}^{m,n} = \iint_{A(m,n)} z_i(x, y) \Delta P_{g,o}^G(x, y) dx dy \quad (13)$$

which can be expanded to the similar form of Eq. (12) where  $\overline{\Delta\Phi_{j,o}^{m,n}}$  and  $a_{j,o}/b_r$  are respectively replaced by  $\overline{\Delta\Phi_{g,o}^{m,n}}$  and  $W_{g,o}/U$ . For the area  $A(m, n)$ , we choose the equally divided box area shown in Fig. 3. If the Mach box, which is a rectangle with diagonals parallel to the Mach lines, is chosen for the box element, the area of  $A(m, n)$  becomes

$$A(m, n) = b_{m,n}^2/\beta = b_c^2/\beta$$

The generalized forces are, therefore, represented in terms of the rigid and elastic airplane responses and the gust excitation, respectively.

The total generalized force due to the loading for the elastic mode becomes

$$Q_{i,j,o}(\omega) = \sum_m \sum_n Q_{i,j,o}^{m,n}(\omega) \quad (14)$$

Similarly, the total generalized force due to loading for the gust excitation is

$$Q_{i,g,o}(\omega) = \sum_m \sum_n Q_{i,g,o}^{m,n}(\omega) \quad (15)$$

Here the summation is carried out over the lifting surfaces only.

## Airplane Response to Continuous Turbulence

### Frequency Response Function

The equations of motion are conveniently formulated from Lagrange's equations by the modal approach. The structure deformation of the airplane is expressed by Eq. (2). The forces acting on the airplane structure are the structural internal forces, aerodynamic response forces, and gust excitation forces.

With the flexible modes chosen to be the natural modes of the free-free airplane vibration, the equations of motion become the following  $N$  simultaneous equations in matrix form:

$$[b_r M_i \{\omega^2 - (1 + ig_i)\omega_i^2\}] \frac{a_{i,o}}{b_r} = [Q_{i,j,o}] \left\{ \frac{a_{j,o}}{b_r} \right\} + \{Q_{i,g,o}\} \frac{W_{g,o}}{U} \quad (16)$$

Solving for  $a_{i,o}$ , the frequency response function is then derived in the following form:

$$H_i(\omega) = \lim_{W_{g,o}/U \rightarrow 1} \left\{ \frac{a_{i,o}(\omega)}{b_r} \right\} = ([b_r M_i \{\omega^2 - (1 + ig_i)\omega_i^2\}] - [Q_{i,j,o}])^{-1} \{Q_{i,g,o}\} \quad (17)$$

where  $Q_{i,j,o}(\omega)$  and  $Q_{i,g,o}(\omega)$  are the elastic response and gust excitation generalized forces due to unit elastic deformation and unit gust angle, respectively, and are obtained from Eqs. (14) and (15).

### Response Loads in the Airplane Structure

Several quantities that define various aspects of the airplane response can be developed from the solution of equations of motion. The frequency response functions can be used to define either the deterministic or the statistical characteristics of the structural response.

Loads at selected elastic axis stations on the airplane are derived by transforming the generalized inertia, damping, and stiffness forces used in the equations of motion into shears, bending moments, and torques for unit deflections of the generalized coordinates. These coefficients are then multiplied by the generalized coordinate frequency response to give the frequency responses of the loads. The set of load equations is written in the following matrix form:

$$\{L\} e^{i\omega t} = [\bar{M}]\{\bar{q}\} + [\bar{C}]\{\dot{q}\} + [\bar{K}]\{q\} + \{\bar{F}_g\} e^{i\omega t} \quad (18)$$

Fig. 3 Dimensions of box area,  $m, n$ .

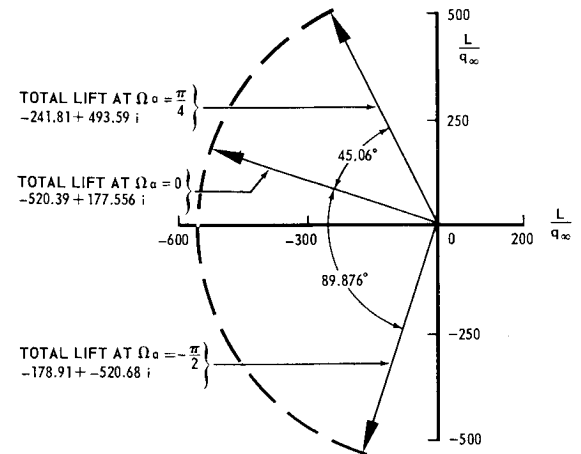
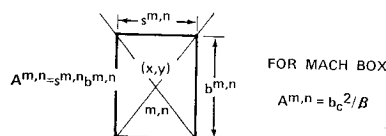


Fig. 4 Orientation of gust force.

Since the airplane system is linear, the following simple relation exists between the spectrum of an input disturbance and the spectrum of the system response:

$$\Phi_0(\Omega) = \Phi_i(\Omega) H(\Omega) \cdot H^*(\Omega) = \Phi_i(\Omega) H(\Omega)^2 \quad (19)$$

The spectral density defines several statistical quantities of interest. The standard deviations of the airplane response quantities are obtained by integrating the spectral density over the range of frequency values,

$$\sigma_y^2 = \int_0^\infty \Phi_y(\Omega) d\Omega \quad (20)$$

$$\sigma_{y'}^2 = \int_0^\infty \Omega^2 \Phi_y(\Omega) d\Omega \quad (21)$$

Similar relations define the other standard deviations and the statistical correlations between any two response quantities. One form of the PSD function of atmospheric turbulence is represented by

$$\Phi(\Omega) = \frac{L \sigma_w^2}{\pi} \frac{1 + (2.6667)(1.339L\Omega)^2}{\{1 + (1.339L\Omega)^2\}^{11/6}} \quad (22)$$

The foregoing analysis of airplane response to atmospheric turbulence considers various response loads, stresses, and accelerations on an individual basis. However, when the airplane encounters atmospheric turbulence, these quantities result simultaneously as interrelated random events. The values of two or more loads should then be considered by the proper statistical combination. In order to provide acceptable approaches from the standpoint of combined statistical requirements, the preceding analysis can easily be extended to determine the combined loads or stresses at a specific point in the structure.<sup>2-5</sup>

## Numerical Examples

Two numerical examples that demonstrate the application of this method are given. First, the method of calculating the gust excitation force is demonstrated for a hypothetical supersonic wing and tail flying at a speed of  $M_\infty = 2.5$  and a cruising altitude = 65,000 ft. The main wing is a 20° untapered, sweptback wing with an aspect ratio of 1.5. The horizontal stabilizer has the leading edge sweptback 25° and has an aspect ratio of 1.3045.

Figure 4 shows the resultant gust excitation forces on main wing due to different gust reference phase angles  $\Omega a$ . The gust spatial frequency is held constant at  $\Omega = 0.01$  rad/ft. As predicted in the foregoing analysis, the resultant gust excitation forces are constant in magnitude and are only rotated around the origin by the amount of initial phase angle  $\Omega a$ . Therefore, for the problem of dynamic

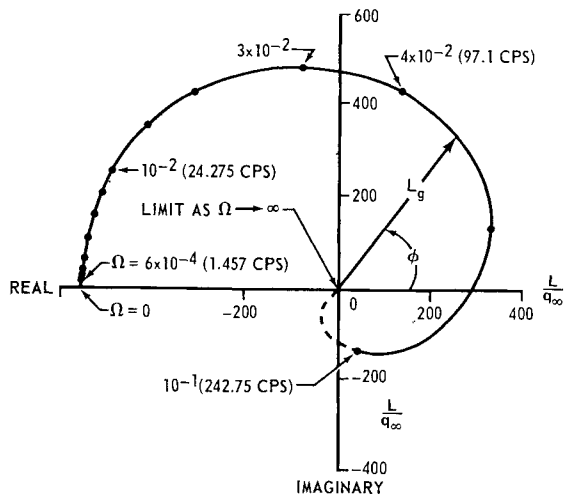


Fig. 5 Gust excitation force vs gust frequency.

gust response, we may simply choose  $\Omega a = 0$ . Thus, the phase angles of the responses of the elastic and rigid generalized coordinates will be referenced to the sinusoidal gust excitation vector located at  $x = 0$ . The resultant excitation forces on main wing due to the variation of gust frequency for a fixed-orientation phase angle  $\Omega a = 0$  are shown in Figs. 5, 6, and 7.

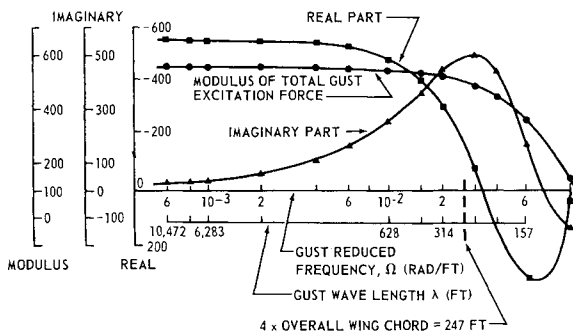


Fig. 6 Wing aerodynamic load vs gust frequency.

The lift distribution, which is the real part of loads, on the main wing and stabilizer is shown in Fig. 8, for a constant gust frequency  $\Omega = 0.01$  rad/ft and  $\Omega a = 0$ . A comparison is made for the stabilizer without the aerodynamic coupling with the main wing under the same gust environment. These results are shown in the dotted line. A certain variation from the wing-coupled case is observed. However, the dif-

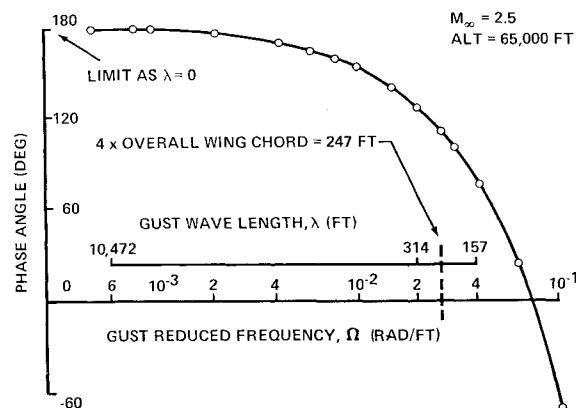


Fig. 7 Phase angle of gust vs gust frequency.

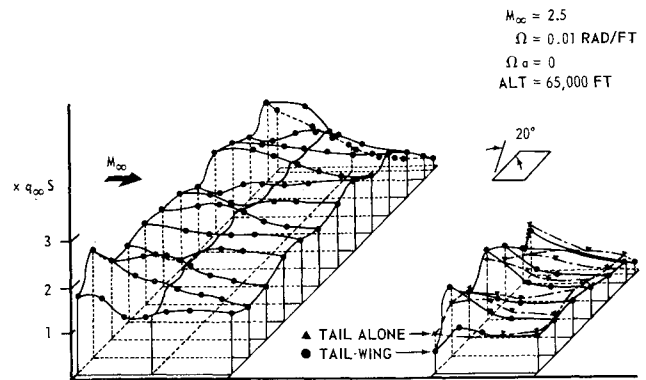


Fig. 8 Real part of pressure due to gust.

ference in the total loads on stabilizer between the two cases is not substantial. The pressure distribution caused by the main wing is varied by the relative location of two wing and stabilizer, their geometries, and gust frequency. Assessment of the design loads on the stabilizer due to gust excitation is obtained by taking account of the aerodynamic influence of both wing and fuselage.

The second numerical example demonstrates the use of this method of gust representation in the power spectral analysis of a large, flexible, supersonic transport. The planform of the airplane analyzed is outlined in Fig. 9. The analysis considers a medium weight cruise configuration with a wing sweep of  $72^\circ$  and flying at an altitude of 61,000 ft and Mach number of 2.7. The dynamic analysis examines six degrees of freedom: the first four symmetric free-free modes plus rigid body vertical translation and pitch. Loads and accelerations are calculated using the gust spectrum of Eq. (22) with a scale of turbulence of 2500 ft. The spectral densities of the bending moment and torque at the wing pivot station are shown in Fig. 10. The effects of the airplane short period and flexible modes are evident, except that the effect of the first flexible mode is absent at this location. The spectral density of the vertical acceleration of the airplane c.g. station is shown in Fig. 11. The corresponding standard deviation (rms level) is  $0.00638g$ 's. This figure clearly indicates the effects of the short period and the flexible modes on the acceleration level.

The acceleration calculation is repeated for an uncoupled case, where the aerodynamic effects of the wing upon the stabilizer are ignored. Thus, the wing and stabilizer are represented separately. No correction factor for wing downwash is used other than to assure that the gust excitation forces are consistently phased. The resulting spectral density for the airplane c.g. acceleration is also shown in Fig. 11. The corresponding rms level is  $0.0095g$ 's.

The comparison demonstrates the very significant difference in acceleration levels that would be predicted by the two methods. The largest difference appears in the first and fourth flexible modes. The change in the tuned response of these modes is due to the introduction of lagged downwash on the stabilizer. In this example, the downwash reduces the short period frequency and increases its damping.

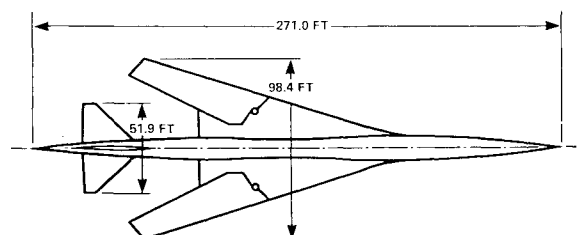
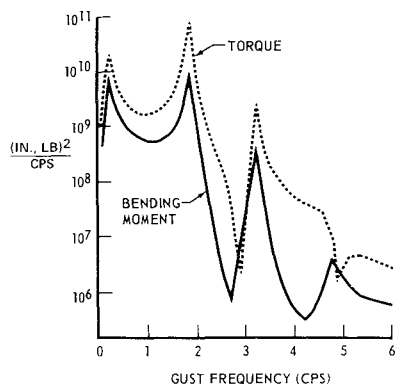


Fig. 9 Planform of supersonic airplane.

**Fig. 10 Spectra of wing pivot bending moment and torque.**

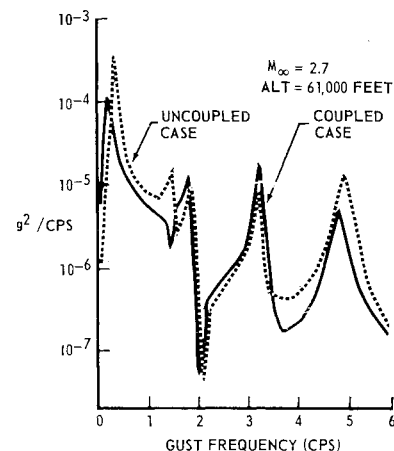


### Concluding Remarks

An analytical evaluation of unsteady aerodynamic forces and dynamic response of a flexible airplane to continuous turbulence in supersonic flight by applying the PSD method has been made. From the foregoing discussions, the following remarks may be summarized:

- 1) The aerodynamic influence coefficients for an airplane with coplanar wings of arbitrary planform subjected to a random vertical turbulence description can be readily computed by the box technique.
- 2) The selection of the gust upwash reference coordinate is arbitrary and only results in a shift of the reference phase angle  $\Omega a$ .
- 3) For a conventional steady-state condition, in the limit as the gust excitation frequency approaches zero, the total excitation force becomes real and is close to the theoretical value for a constant angle of attack.
- 4) As gust excitation frequency increases, the total gust excitation force monotonically decreases both in magnitude and phase angle, Figs. 6 and 7. However, when the gust wavelength approaches 4 times the over-all wing chord (streamwise length between the foremost leading-edge and aftermost trailing-edge points on the wing), the rate of change in both force magnitude and phase angle increases. Since the gust wavelengths of interest are mostly in the monotonical variation range, the method of interpolation for calculating the gust excitation force can be used.
- 5) As gust excitation frequency becomes very large (gust wavelength is less than over-all wing chord), the total excitation force quickly decreases and vanishes in the limit. However, when the gust wavelength becomes less than four times the box chord dimension, the box technique is invalid.
- 6) The aerodynamic coupling effect of the main wing on the stabilizer should not be ignored. The extent of the effect

**Fig. 11 Spectrum of airplane c.g. acceleration.**



is a function of airplane geometry, flight Mach number, and gust excitation frequency and is most noticeable on the responses of the airplane pitch and flexible body modes.

### References

- <sup>1</sup> Evvard, J. C., "Use of Source Distributions for Evaluating Theoretical Aerodynamics of Thin Finite Wings at Supersonic Speeds," Rept. 951, June 1949, NACA.
- <sup>2</sup> Fuller, J. R., "Strength Margins for Combined Random Stresses," Doc. D6-2561TN, Oct. 1964, The Boeing Co., Seattle, Wash.
- <sup>3</sup> Fuller, J. R. et al., "Contributions to the Development of a Power-Spectral Gust Design Procedure for Civil Aircraft," FAA-ADS-54, Jan. 1966, The Boeing Co., Renton, Wash.
- <sup>4</sup> Houbolt, J. C., Steiner, R., and Pratt, K. G., "Dynamic Response of Airplanes to Atmospheric Turbulence Including Flight Data on Input and Response," TR R-199, 1964, NASA.
- <sup>5</sup> Hoblit, F. M. et al., "Development of Power-Spectral Gust Design Procedure for Civil Aircraft," FAA-ADS-53, Jan. 1966, Lockheed-California Co., Sunnyvale, Calif.
- <sup>6</sup> Li, J. M. and Briscoe, B., "Calculation of Unsteady Aerodynamic Forces and Dynamic Response of Flexible Aircraft Structure to Continuous Turbulence in Supersonic Flight," Doc. D6-10977TN, Aug. 1966, The Boeing Co., Seattle, Wash.
- <sup>7</sup> Pines, S., Dugundji, J., and Neuringer, J., "Aerodynamic Flutter Derivatives for a Flexible Wing with Supersonic and Subsonic Edges," *Journal of the Aerospace Sciences*, Vol. 22, No. 10, Oct. 1955, pp. 693-700.
- <sup>8</sup> Weatherill, W. H., and Mimmack, J. J., "An IBM 7090 Program for Calculating Unsteady Airlloads on Arbitrary Lifting Planforms in Supersonic Three-Dimensional Flow," Doc. D2-12281, Nov. 1962, The Boeing Co., Seattle, Wash.